DENTAL MATERIALS 35 (2019) 1450–1463

Available online at www.sciencedirect.com

ScienceDirect

journal homepage: www.intl.elsevierhealth.com/journals/dema

Does recharging dental restorative materials with fluoride influence biofilm formation?

Andrei Ionescu[a], *Eugenio Brambilla*[a], *Sebastian Hahnel*[b,*]

[a] *Department of Biomedical, Surgical and Dental Sciences, University of Milan, Italy*
[b] *Poliklinik für Zahnärztliche Prothetik und Werkstoffkunde, Leipzig University, Leipzig, Germany*

ARTICLE INFO

Keywords:
Biofilm
Resin-based composite
Bioreactor
Fluoride
Glass ionomer cement
Streptococcus

ABSTRACT

Objectives. To investigate the influence of recharging dental restorative materials with fluoride on biofilm formation.

Methods. Specimens produced from a high-viscosity glass ionomer cement (HVGIC), a resin-modified glass ionomer cement (RMGIC), and a resin-based composite (RBC) were randomly allotted to incubation in artificial saliva either for one week (AS-1), for five weeks (AS-5), for five weeks including twice/day brushing with 1450 ppm NaF toothpaste (AS-5-brush), or one-time exposition to 5000 ppm NaF after five weeks of incubation (AS-5-exp). Human enamel was used as reference. Surface roughness and the release of fluoride from the specimens was determined; biofilm formation was simulated using mono- or multispecies microbiological models and analysed employing an MTT-based approach and confocal laser-scanning microscopy.

Results. Monospecies biofilm formation was significantly reduced on HVGIC in comparison to RMGIC and RBC. It was also reduced on HVGIC and enamel after treatment with fluoride in groups AS-5-brush and AS-5-exp in comparison to AS-5. These effects were particularly pronounced after 24 h, and less pronounced after 48 h of biofilm formation. In the multispecies microbiological model, similar observations were identified for HVGIC, while for enamel a significant reduction in biofilm formation was observed in groups AS-5-brush and AS-5-exp. No significant effect of fluoride treatments was identified for RMGIC and RBC, regardless of the microbiological model applied.

Significance. These data indicate that biofilm formation on the surfaces of a glass ionomer cement and enamel can be relevantly influenced by treatment with fluoride. Enamel may serve as a fluoride reservoir which requires regular recharge.

1. Introduction

Regardless of the restorative material employed, secondary caries is still one of the most frequent reasons for failure of dental restorations. It is closely related to the presence of cariogenic biofilms on the surface of a dental restoration [1]. A relevant part of contemporary dental research deals with the development and analysis of restorative materials with low susceptibility to adhere cariogenic microorganisms,

* *Corresponding author at*: Poliklinik für Zahnärztliche Prothetik und Werkstoffkunde, Universitätsklinikum Leipzig, Liebigstraße 12, Haus 1 04103 Leipzig, Germany.
E-mail address: sebastian.hahnel@medizin.uni-leipzig.de (S. Hahnel).

https://doi.org/10.1016/j.dental.2019.07.019
0109-5641/

which aims to improve the survival rates of dental restorations. Glass ionomer cements (GICs) micromechanically and chemically adhere to tooth tissues and release fluoride and other ions such as sodium, phosphate, and silicate [2–5]. While GICs were initially used as provisional restorative materials, modern high-viscosity GICs can also be employed for the fabrication of permanent restorations. Due to their chemical properties, GICs interact with both natural tooth tissues and the biofilm on their surface, which is why they can be regarded as bioactive materials. Regarding the influence of fluoride released from restorative materials on biofilm formation on their surface, GICs feature a fluoride burst effect, implying that the release of fluoride from these materials is initially high and decreases rapidly with time [6]. This phenomenon suggests that restorative materials may only initially modulate development and properties of biofilms on their surface.

While it has been controversially discussed whether the levels of fluoride released from GICs are too low for having a relevant impact on oral biofilms [7], several laboratory and clinical studies have identified less biofilm formation on the surface or in the direct proximity of GICs [8,9]. A recent study suggested a significant correlation between the levels of fluoride released from GICs and the biochemical and physical properties of *Streptococcus mutans* biofilms on the surface of these materials [10]. However, investigations from our groups indicated that the correlation between these variables is not as simple, since the release of fluoride is not the only parameter modulating *S. mutans* biofilm formation on these materials. Nevertheless, our studies corroborated the impact of fluoride released from GICs on biofilms and indicated that the impact of fluoride on *S. mutans* biofilm formation was particularly pronounced in the early periods of biofilm formation. Correlations with surface properties such as roughness or surface free energy, which are commonly employed to explain biofilm formation, were poor [11,12]. Previous studies highlighted that GICs can be effectively recharged with fluoride-containing solutions or toothpastes [13,14], yet the effect of recharging dental restorative materials with fluoride on biofilm formation on their surface has, to the knowledge of the authors, never been addressed. Thus, the aim of the present laboratory study was to investigate the impact of recharging several restorative dental materials with fluoride on *S. mutans* and multispecies biofilm formation. The study hypotheses were that (1) recharging restorative materials with fluoride decreases biofilm formation on their surface, and (2) this effect is dependent on time, biofilm, and material.

2. Materials and methods

2.1. Specimen preparation

Standardized specimens were prepared from a high-viscosity GIC (HVGIC), a resin-modified GIC (RMGIC), and a conventional resin-based composite (RBC) (Table 1). For preparation of a single specimen, a standardized amount of each material was placed into a custom-made steel mould with a diameter of 6.0 mm and a height of 2.0 mm, covered with a cellulose acetate strip (Mylar®), and condensed against a glass plate until cured. RMGIC and RBC specimens were light-cured in direct contact for 40 s using a hand-held light curing unit (SDI Radii plus, SDI, Bayswater, Australia; 1500 mW/cm^2).

Anterior human teeth that had been extracted for clinical reasons were obtained from the Oral Surgery Unit at the Department of Biomedical, Surgical and Dental Sciences (Milan, Italy), immediately frozen after extraction, and thawed before use. Round enamel slabs with a diameter of 6.0 mm and a thickness of 2.0 mm were cut from the labial surfaces using a water-cooled trephine diamond bur (INDIAM, Carrara, Italy) and were then stored in artificial saliva.

All specimens were subjected to a standardized polishing protocol, including polishing with 1000/4000-grit grinding paper (Buehler, Lake Bluff, IL, USA) in a polishing machine (Motopol 8; Buehler, Düsseldorf, Germany), and were subsequently stored under light-proof conditions in artificial saliva for one week at 37 ± 1 °C prior to further processing; this procedure allowed maturation of the cement and minimized potential effects of an initial fluoride burst and residual monomers leakage on microbiological procedures. The artificial saliva simulated the average electrolyte composition of human whole saliva and was prepared from 0.1 L of 150 mM $KHCO_3$, 0.1 L of 100 mM NaCl, 0.1 L of 25 mM K_2HPO_4, 0.1 L of 24 mM Na_2HPO_4, 0.1 L of 15 mM $CaCl_2$, 0.1 L of 1.5 mM $MgCl_2$ and 0.006 L of 25 mM citric acid. The volume was made up to 1 L and pH was adjusted to 7.0 by pipetting 4 M NaOH or 4 M HCl solutions under vigorous stirring [15].

All specimens were then cleaned using distilled water and applicator brush tips (3 M ESPE, Seefeld, G).

2.2. Study design

The specimens were randomly allotted to four groups with different treatment protocols (cf. Fig. 1). The artificial saliva in groups AS-5, AS-5-brush, and AS-5-exp was exchanged twice each day to simulate a prolonged ageing effect and a continuous washout of fluoride. Subsequently, the specimens were forwarded to surface analysis and simulation of biofilm formation.

2.3. Surface characteristics

2.3.1. Surface roughness

Peak-to-valley surface roughness (R_a) was determined on five randomly selected specimens for each material and treatment group using a profilometric contact surface measurement device (Surtronic 3+, Taylor-Hobson, Leicester, UK). A distance of 1.75 mm was measured in three randomly selected line scans perpendicular to the expected grinding grooves using a standard diamond tip (tip radius 2 μm, tip angle 90°) and a cut-off level of 0.25.

2.3.2. Scanning electron microscopy and electron-dispersive X-ray spectroscopy (SEM-EDS)

SEM-EDS analyses were performed on five specimens for each group using a tabletop scanning electron microscope (TM4000Plus; Hitachi, Schaumburg, IL, USA) equipped with an EDS probe (Q75, Bruker, Berlin, Germany). Dry specimens were mounted on stubs using conductive tape and were analyzed without sputter-coating, using both a secondary electron (SE) detector and an accelerating voltage of 5 kV in surface-charge

Table 1 – Materials used in the current study.

Name	Type	Abbreviation	Manufacturer	Composition
Ionostar plus	high-viscosity glass ionomer cement	HVGIC	VOCO, Cuxhaven, Germany	F – Al - Si glass; polyacrylic acid, tartaric acid
Ionolux	Resin-modified glass ionomer cement	RMGIC		F – Al - Si glass; polyacrylic acid, resin monomers
GrandioSo	Resin-based composite	RBC		Resin: Bis-GMA, Bis-EMA, TEGDMA, camphorquinone, butylated hydroxytoluene. Filler: glass ceramic filler with an average particle size of 1 micrometer; functionalized silicon dioxide nanoparticles with a size of 20 –40 nm; pigments (iron oxide, titanium dioxide)
Human enamel		Enamel	N/A	

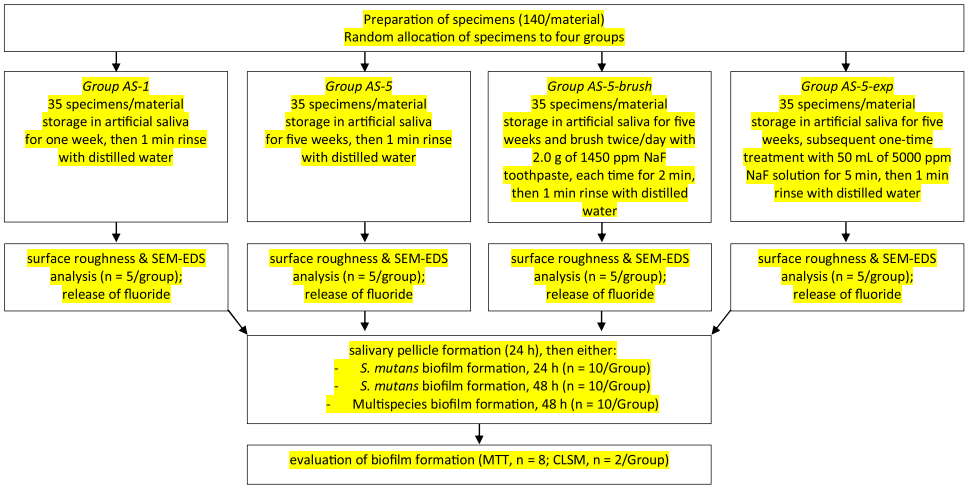

Fig. 1 – Flow chart of the study design.

reduction mode to provide information from a ≈500 nm superficial layer, and a backscattered electron (BE) detector and an accelerating voltage of 15 KV in normal vacuum conditions. The latter conditions were also employed for EDS analyses. Three randomly selected fields were acquired for each specimen in SE mode (300×, 5000×), in BE mode (300×, 5000×), and with the EDS probe at 300x in full-frame mode using an acquisition time of 150 s. Elemental distribution at the surface was obtained in map mode (2000×–10,000×) using an acquisition time of 600 s. EDS data rendered the elemental composition of the superficial layer of the analyzed specimen (≈1–1.5 μm).

2.4. *Microbiological procedures*

2.4.1. *Saliva preparation*

Whole saliva was collected from five healthy volunteers in accordance with a previously published protocol [16]. The volunteers gave their informed consent to participate and refrained from oral hygiene for 24 h, did not have any active dental disease, and did not have antibiotic therapy for at least 3 months prior to the experiments. Chilled test tubes were used for saliva collection. For simulation of salivary pellicle formation, saliva from the various donors was pooled, heated to 60 °C for 30 min, and centrifuged (12,000× *g*, 4 °C, 15 min). The supernatant was transferred into sterile tubes, stored at −20 °C, and thawed at 37 °C for 1 h prior to the experiments. To provide an inoculum for the multispecies microbiological model, saliva was analogously collected and pooled from the five donors, yet was immediately used to inoculate the bioreactor.

2.4.2. *Bacteria*

S. mutans ATCC 35668 was cultured in accordance with a previously published protocol [17]. Briefly, Mitis Salivarius Bacitracin agar inoculated plates were incubated in a 5% supplemented CO_2 environment at 37 °C for 48 h. A total of 1 wt% sucrose was added to a pure suspension of the microorganism in Brain Heart Infusion obtained from these plates after overnight incubation in a 5% supplemented CO_2 environment at 37 °C. *S. mutans* cells were harvested by centrifugation (2200× *g*, 19 °C, 5 min), washed twice with phosphate-buffered saline (PBS), and resuspended. The suspension was subsequently subjected to low intensity ultrasonic energy (Sonifier model B-150; Branson, Danbury, CT, USA; operating at 7-W energy output for 30 s) in order to disperse bacterial chains. The suspension was then adjusted to a value of 1.0 on the McFarland scale, corresponding to a microbial concentration of approximately 6.0×10^8 cells/mL.

2.4.3. *Biofilm formation*

A total of 30 specimens for each material and group (AS-1, AS-5, AS-5-brush, AS-5-exp) were randomly allocated to three different microbiological models (n = 10 for each material and group, one round/microbiological model), including a monospecies microbiological model with *S. mutans* and either 24 h or 48 h of incubation or a multispecies microbiological model employing pooled whole saliva and 48 h of incubation.

For simulation of biofilm formation, a modification of a commercially available Drip Flow Reactor (DFR 110; Biosurface Technologies, Bozeman, MT, USA) was employed. The modified design allowed the placement of customized specimen-trays on the bottom of the flow cells and the complete immersion of the surfaces of the specimens into the surrounding flowing medium [18]. Specimens were randomly distributed across eight Teflon trays, which fixed the specimens tightly and exposed their surfaces to the surrounding medium; the trays were press-fitted on the bottom of each flow cell of the reactor. All tubing and specimen-containing trays were sterilized prior to the experiments using a chemiclave with hydrogen peroxide gas plasma technology (Sterrad; ASP, Irvine, CA, USA). Heat-related damage of the specimens was avoided by limiting the maximum temperature to 45 °C. The whole reactor was assembled inside a sterile hood and transferred into a thermostat to operate under a standardized temperature of 37 °C.

For simulation of salivary pellicle formation, the surfaces of the specimens in each flow cell were exposed to thawed sterile saliva for 24 h. Simulation of monospecies biofilm formation was initiated by inoculating 10 mL of *S. mutans* suspension into each flow cell of the first two bioreactors. For simulation of multispecies biofilm formation, 10 mL of pooled human whole saliva were immediately inoculated into each flow cell of the third bioreactor. After 4 h of incubation under static conditions to allow adherence and initial colonization of the surfaces, a multichannel, computer-controlled peristaltic pump (RP-1; Rainin, Emeryville, CA, USA) was used to provide a constant flow of nutrient broth through all flow cells for the specified incubation time. The sterile nutrient broth was enriched with 10.0 g/L sucrose and consisted of 2.5 g/L mucin (type II, porcine gastric), 2.0 g/L bacteriological peptone, 2.0 g/L tryptone, 1.0 g/L yeast extract, 0.35 g/L NaCl, 0.2 g/L KCl, 0.2 g/L CaCl2, 0.1 g/L cysteine hydrochloride, 0.001 g/L hemin, and 0.0002 g/L vitamin K1. The flow rate was set to 9.6 mL/h [17].

2.4.4. *Viable biomass assessment*

Subsequent to either 24 h or 48 h of incubation in the mono- or multispecies microbiological model, viable biomass adherent to the specimens' surfaces was assessed with a MTT-based assay [18]. In brief, MTT stock solution was prepared by dissolving 5 mg/mL 3-(4,5)-dimethylthiazol-2-yl-2,5-diphenyltetrazolium bromide in sterile PBS; phenazine methosulfate (PMS) stock solution was prepared by dissolving 0.3 mg/mL of N-methylphenazinium methyl sulphate in sterile PBS. The solutions were stored at 2 °C in light-proof vials until the day of the experiment, when a fresh measurement solution (FMS) was prepared by diluting 1:10 v/v of MTT stock solution and 1:10 v/v of PMS stock solution in sterile PBS. A lysing solution (LS) was prepared by dissolving 10% v/v of sodium dodecyl sulphate and 50% v/v dimethylformamide in deionized water.

Subsequent to either 24 h or 48 h of incubation in the mono- or multispecies microbiological model, the flow of nutrient broth was stopped, the flow cells were opened, and the trays containing the specimens were carefully removed and immediately placed in Petri dishes with sterile PBS at 37 °C. The specimens were subsequently gently removed from the tray, passed into another dish with sterile PBS at 37 °C to remove non-adhered cells, and finally transferred into 48-well plates. 300 μl of FMS solution were added to each well, and the plates were incubated for 3 h at 37 °C under lightproof conditions. During incubation, electron transport across the microbial plasma membrane and, to a lesser extent, microbial redox systems converted the yellow salt to insoluble purple formazan crystals. The conversion at the cell membrane level was facilitated by the intermediate electron acceptor (PMS). The unreacted FMS solution was gently removed, and the formazan crystals were dissolved by adding 300 μL of LS to each well. The plates were stored for an additional hour under lightproof conditions at room temperature; 100 μL of the solution were then transferred into the wells of 96-well plates. The absorbance of the solution was measured using a spectrophotometer (Genesys 10-S, Thermo Spectronic, Rochester, NY, USA) at a wavelength of 550 nm, and the results were displayed as optical density (OD) units.

2.4.5. *Confocal laser-scanning microscopy*

A total of two specimens for each material and treatment group were gently removed from the flow cells, rinsed twice with sterile PBS, stained using the FilmTracer™ LIVE/DEAD® Biofilm Viability Kit (Invitrogen Ltd., Paisley, UK), and analyzed using confocal laser-scanning microscopy (CLSM; Leica TCS SP2, Leica Microsystems, Wetzlar, Germany). Four randomly selected image stack sections were recorded for each specimen and incubation time. Confocal images were obtained using a dry objective (20×; NA = 0.7) and digitalized using the Leica Application Suite Advanced Fluorescence Software (LAS-AF, Leica Microsystems) at a resolution of 2048 × 2048 pixels, with a zoom factor of 1.0 and a scan speed of 400 Hz. Three channels were acquired; one featured an excitation at 405 nm and emission at 420–470 nm in order to digitally subtract potential autofluorescence. The other two channels had an excitation wavelength of 488 nm and emission was acquired at 500–570 nm (green channel, live bacteria) and 610–760 nm (red channel, dead bacteria). For each image stack section, 3D-rendering reconstructions were obtained using ImageJ (National Institutes of Health, Bethesda, MD, USA) and Drishti (Ajay Limaye, Australian National University, CAN, AUS http://sf.anu.edu.au/Vizlab/drishti/).

2.5. *Determination of the release of fluoride*

The release of fluoride from each material was determined prior to simulation of biofilm formation. The artificial saliva storage medium from each treatment group was collected during one week, which accounted for an overall total of four measurements for groups AS-5 and AS-5-brush. Measurements in group AS-1 produced baseline values for all groups after the first week of storage in artificial saliva. Due to the

analogous storage protocol in group AS-5-exp as in group AS-5, AS-5-exp was not measured separately. Recharge with fluoride in specimens in group AS-5-exp was identified by analyzing the 5000 ppm fluoride solutions following exposure to the various specimens. The amount of fluoride that had been absorbed by the specimens was calculated from the difference between the original and residual amount of fluoride in the solution. The absorbed amount of fluoride was calculated and displayed in ppm/mm^2 of the surface of the corresponding material. This procedure allowed the calculation of a kinetic function regarding the release of fluoride from HVGIC and RMGIC in artificial saliva prior to, and after treatment with fluoride in groups AS-5-brush and AS-5-exp.

All analyses were performed using the ion-selective electrode micro-method, as described previously [11]. In brief, a stock solution with a fluoride concentration of 1000 ppm was appropriately diluted with artificial saliva to obtain fluoride standards with fluoride concentrations ranging from 0.0019 to 64 parts per million (ppm). A calibration curve was obtained by measuring fluoride standards using a digital pH/mV meter (SA-720, Orion Research Inc, Boston, MA, USA). Sodium acetate buffer 20% v/v with EDTA as ionic strength adjustor was added to each standard prior to the analyses. A negative reference standard (0 ppm fluoride) was prepared by adding 20% v/v of sodium acetate buffer with EDTA to the artificial saliva; this solution was also used to rinse the electrodes between the single measurements.

2.6. *Statistical analysis*

Statistical analyses were performed using JMP 10.0 software (SAS Institute, Cary, NC, USA). Normal distribution of data was checked using Shapiro–Wilk's test and homogeneity of variances was verified using Levene's test. Means and standard errors were calculated from the raw data. Surface roughness data were log-transformed prior to statistical analysis to approach normal distribution. Two-way analysis of variance (ANOVA) was employed to analyse surface roughness, EDS, and viable biomass data, considering "material" and "treatment" as fixed factors. Release of fluoride was analysed using three-way ANOVA, setting "material", "treatment", and "time point" as fixed factors. Tukey's test was applied for post-hoc analyses. The level of significance (α) was set to 0.05.

3. Results

3.1. *Surface analyses*

Details on the surface roughness of the various materials and specimens are displayed in Fig. 2. Significant differences were identified between the materials (HVGIC > RMGIC ($p = .035$), RMGIC = enamel ($p = .113$), enamel > RBC ($p = .005$). The various treatments had no influence on the roughness of the RMGIC, while storage in artificial saliva slightly increased the surface roughness of HVGIC and RBC and decreased the surface roughness of enamel. Brushing with toothpaste in group AS-5-brush led to a slight decrease of surface roughness for RBC and HVGIC compared to the other groups.

HVGIC and RMGIC appeared very similar in the SEM analyses (Fig. 3, AS-1), featuring sharp particles of a few microns embedded into a lighter matrix. RMGIC appeared to have more tightly packed filler particles and fewer cracks and bubbles than HVGIC. For all materials, parallel grooves caused by the polishing procedures were identified. The RBC showed a very homogeneous surface with filler particles ranging from micro- to nanoscale embedded into a resin matrix. Characteristic prismatic structures were identified for enamel in backscattered electron mode.

After 5 weeks of storage (AS-5), fewer cracks were identified on the surface of HVGIC and RMGIC. Treatment with the highly concentrated fluoride solution (group AS-5-exp) did not produce relevant differences in the morphology of the surfaces. Tooth brushing (group AS-5-brush) produced distinct changes in the appearance of the surface of HVGIC and, especially, RMGIC. For RMGIC, brushing removed filler particles in the surface which caused an exposition of the matrix. For RBC and enamel surfaces, no modifications were identified.

Table 2 indicates the surface composition of the various materials after the different treatments, as acquired by EDS. Storage time correlated with a significant decrease in the level of surface fluoride for HVGIC and RMGIC. Treatment with fluoride in groups AS-5-brush and AS-5-exp coincided with a significant increase in surface fluoride for these materials, as well as enamel. Treatment in group AS-5-exp produced higher levels of surface fluoride in HVGIC compared to baseline and to AS-5-brush, while treatment in group AS-5-brush produced higher levels of surface fluoride in enamel when compared to AS-5-exp. Treatment in group AS-5-brush produced accumulation of titanium on the surface of HVGIC, RMGIC, and enamel.

As titanium is one of the ingredients of the toothpaste (Table 2), EDS maps (Fig. 4) proved a transfer of titanium from the toothpaste to the surface of HVGIC, RMGIC, and enamel after brushing (group AS-5-brush); no titanium was identified on the surfaces of the RBC.

3.2. *Biofilm formation*

Fig. 5a displays the results for monospecies *S. mutans* biofilm formation after 24 h. Both factors, material and treatment, significantly influenced biofilm formation ($p < 0.001$). Viable biomass on HVGIC slightly increased after extended incubation in artificial saliva (group AS-5) in comparison to baseline (group AS-1); treatments in group AS-5-brush and AS-5-exp led to a significant reduction in viable biomass in comparison to the reference group AS-1 ($p < 0.05$). No significant differences in viable biomass were identified for RMGIC and RBC, indicating that treatments in group AS-5-brush and AS-5-exp had no relevant effect on monospecies biofilm formation on the surface of these materials. For enamel, both groups AS-5-brush and AS-5-exp showed a significant decrease in viable biomass ($p < 0.005$).

Fig. 5b displays the results for monospecies *S. mutans* biofilm formation after 48 h. Fewer differences in viable biomass between the materials and groups were identified than after 24 h, and no effect of fluoride-releasing materials on viable biomass was observed. Nevertheless, the effect of treatment with fluoride in groups AS-5-brush and AS-5-exp

Table 2 – Surface elemental composition (wt%) of the various materials immediately after polishing procedures (T = 0) and after the different treatment protocols as identified by energy-dispersive X-ray spectroscopy (EDS). Data identified for O, Na, Mg, and K are not displayed. Different letters indicate statistically significant differences between groups (Tukey test, $p < 0.05$).

		C		F		Al		Si		P		Ba		Sr		Ca		Ti		Inorg.	
HVGIC	T = 0	20.97 (1.26)	c,d,e	7.13 (0.21)	a,b	8.22 (0.30)	a	8.00 (0.63)	c,d	1.44 (0.07)	f,g,h,i	0.00 (0.00)	e	8.97 (0.90)	b,c,d	0.00 (0.00)	e	0.00 (0.00)	b	34.82 (1.88)	d,e
	AS-1	20.22 (0.35)	b,c,d,e,f	5.15 (0.10)	c	8.44 (0.07)	a	8.76 (0.06)	c	1.44 (0.03)	f,g,h,i	0.00 (0.00)	e	9.17 (0.15)	a,b,c,d	1.69 (0.16)	c,d,e	0.00 (0.00)	b	34.11 (0.02)	d,e,f
	AS-5	18.98 (2.30)	c,d,e,f,g	3.93 (0.30)	c	8.22 (0.37)	a	7.12 (0.79)	d,e	3.70 (1.49)	d,e	0.00 (0.00)	e	9.95 (0.05)	a,b,c	4.61 (1.58)	c,d	0.00 (0.00)	b	34.10 (0.06)	d,e,f
	AS-5-brush	18.17 (0.24)	c,d,e,f,g	5.84 (1.02)	b,c	8.25 (0.21)	a	9.14 (0.28)	c	1.91 (0.24)	e,f,g,h	0.00 (0.00)	e	8.24 (0.01)	c,d	2.89 (0.77)	c,d,e	0.27 (0.05)	a,b	34.49 (0.74)	d,e,f
	AS-5-exp	19.68 (1.69)	c,d,e,f	8.30 (1.28)	a	8.00 (0.36)	a	7.37 (0.54)	d,e	2.48 (0.54)	d,e,f	0.00 (0.00)	e	9.28 (0.24)	b,c,d	4.87 (1.49)	c	0.00 (0.00)	b	36.59 (0.94)	c,d,e
RMGIC	T = 0	28.40 (0.77)	a,b	5.62 (0.51)	b,c	7.76 (0.17)	a	8.13 (0.23)	c,d	2.05 (0.16)	e,f,g	0.00 (0.00)	e	9.77 (1.07)	a,b,c	0.30 (0.15)	e	0.00 (0.00)	b	34.13 (1.51)	e,f
	AS-1	25.64 (0.41)	a,b,c,d	5.82 (0.07)	b,c	8.01 (0.07)	a	7.97 (0.09)	c,d	2.37 (0.05)	d,e,f,g	0.00 (0.00)	e	10.14 (0.14)	a,b,c	0.49 (0.08)	e	0.00 (0.00)	b	35.27 (0.35)	c,d,e,f
	AS-5	23.35 (0.51)	b,c,d,e	5.36 (0.22)	b,c	7.55 (0.23)	a,b	7.11 (0.21)	d,e	4.01 (0.18)	d	0.00 (0.00)	e	10.81 (0.08)	a,b	1.64 (0.68)	c,d,e	0.00 (0.00)	b	36.09 (0.42)	c,d,e
	AS-5-brush	32.43 (8.93)	a	4.62 (1.30)	c	6.25 (1.17)	b	6.50 (0.62)	e	2.44 (0.68)	d,e,f	0.00 (0.00)	e	7.97 (1.36)	d	2.33 (1.05)	c,d,e	0.58 (0.62)	a	28.59 (2.22)	f
	AS-5-exp	26.57 (1.12)	a,b,c	7.16 (0.66)	a,b	7.68 (0.32)	a	7.36 (0.43)	d,e	2.68 (0.14)	d,e,f	0.00 (0.00)	e	10.92 (0.29)	a	1.80 (0.53)	d,e	0.00 (0.00)	b	36.92 (0.53)	c,d,e
RBC	T = 0	13.62 (0.51)	f,g,h,i	0.00 (0.00)	e	3.44 (0.08)	c	24.35 (0.33)	a	0.00 (0.00)	i	14.02 (0.46)	a	0.00 (0.00)	e	0.09 (0.06)	e	0.00 (0.00)	b	41.81 (0.77)	c
	AS-1	13.99 (0.68)	e,f,g,h,i	0.07 (0.03)	e	3.69 (0.06)	c	23.94 (0.66)	a,b	0.02 (0.02)	h,i	13.20 (0.05)	b	0.00 (0.00)	e	0.16 (0.07)	e	0.00 (0.00)	b	40.91 (0.71)	c,d,e
	AS-5	14.77 (0.56)	e,f,g,h,i	0.18 (0.00)	e	3.59 (0.06)	c	22.51 (0.09)	b	0.29 (0.31)	g,h,i	11.79 (0.72)	d	0.00 (0.00)	e	0.51 (0.41)	e	0.00 (0.00)	b	38.49 (0.25)	c,d,e
	AS-5-brush	14.15 (0.18)	e,f,g,h,i	0.11 (0.00)	e	3.70 (0.02)	c	23.89 (0.19)	a,b	0.03 (0.04)	h,i	13.16 (0.19)	b	0.00 (0.00)	e	0.15 (0.03)	e	0.03 (0.03)	b	41.00 (0.07)	c,d,e
	AS-5-exp	14.97 (0.22)	e,f,g,h	0.57 (0.05)	d,e	3.61 (0.03)	c	23.71(0.16)	a,b	0.03 (0.02)	i	12.45(0.24)	c	0.00 (0.00)	e	0.31 (0.09)	e	0.00 (0.00)	b	40.38 (0.23)	c,d
Enamel	T = 0	7.01 (0.78)	i	0.02 (0.02)	e	0.08 (0.04)	d	0.20 (0.19)	f	14.76 (0.66)	a	0.00 (0.00)	e	0.00 (0.00)	e	35.40 (0.79)	a	0.00 (0.00)	b	50.46 (1.23)	a,b
	AS-1	11.69 (0.83)	f,g,h,i	0.06 (0.01)	e	0.06 (0.01)	d	0.10 (0.02)	f	12.29 (0.95)	b,c	0.00 (0.00)	e	0.00 (0.00)	e	30.24 (2.21)	b	0.00 (0.00)	b	43.24 (3.27)	b,c
	AS-5	17.11 (0.99)	d,e,f,g	0.01 (0.01)	e	0.09 (0.06)	d	0.30 (0.01)	f	11.00 (1.62)	c	0.00 (0.00)	e	0.00 (0.00)	e	27.19 (3.23)	b	0.00 (0.00)	b	39.52 (5.53)	c,d,e
	AS-5-brush	7.55 (1.07)	h,i	0.89 (0.10)	d	0.08 (0.06)	d	0.38 (0.18)	f	14.05 (0.99)	a,b	0.00 (0.00)	e	0.00 (0.00)	e	34.88 (1.64)	a	0.26 (0.27)	a,b	51.09 (2.71)	a
	AS-5-exp	10.29 (1.76)	g,h,i	0.36 (0.08)	e	0.05 (0.03)	d	0.23 (0.11)	f	14.03 (0.19)	a,b	0.00 (0.00)	e	0.00 (0.00)	e	34.25 (1.29)	a	0.00 (0.00)	b	49.47 (1.52)	a,b
Toothpaste		31.29 (4.45)		0.30 (0.29)		0.02 (0.13)		7.15 (1.18)		0.00 ()		0.00 (0.00)		0.00 (0.00)		0.00 (0.00)		1.52 (1.61)		10.05 (1.72)	

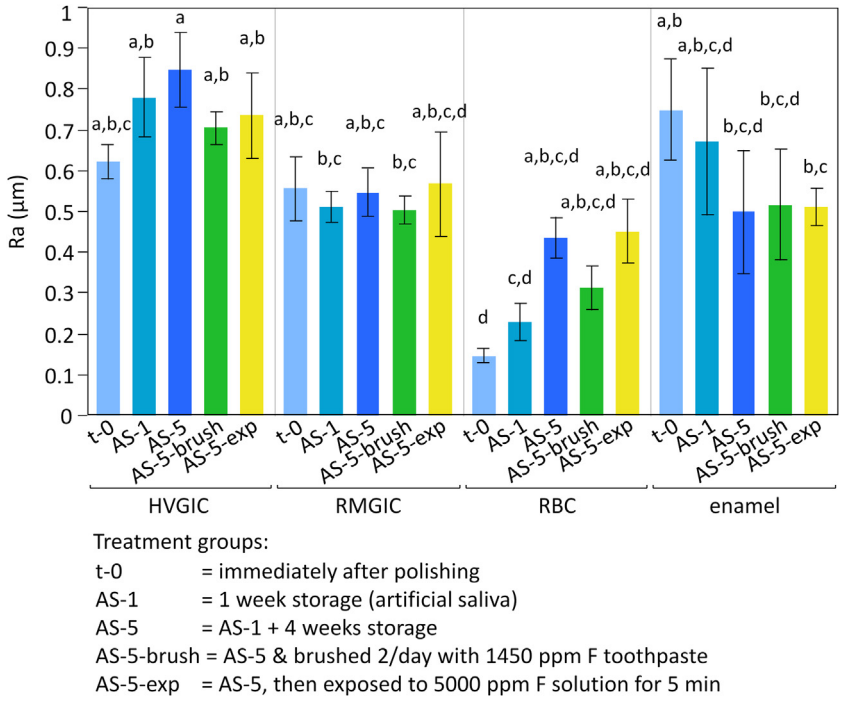

Treatment groups:
t-0 = immediately after polishing
AS-1 = 1 week storage (artificial saliva)
AS-5 = AS-1 + 4 weeks storage
AS-5-brush = AS-5 & brushed 2/day with 1450 ppm F toothpaste
AS-5-exp = AS-5, then exposed to 5000 ppm F solution for 5 min

Fig. 2 – Surface roughness of the various materials after the different treatment protocols. Different letters indicate statistically significant differences between groups (Tukey test, $p < 0.05$).

was still evident. Both factors, material and treatment, significantly influenced viable biomass ($p = 0.009$ and $p = 0.005$, respectively), although no significant interactions were identified. For HVGIC and RBC, slightly lower viable biomass was observed than for enamel ($p < 0.05$). Both fluoride treatments (groups AS-5-brush and AS-5-exp) showed significantly less viable biomass was identified in comparison to the other two groups ($p < .01$).

CLSM analyses conducted for *S. mutans* biofilms after 48 h (Fig. 6) indicated that both material and treatment affected the viability and morphology of the biofilms. After 1 week of storage (group AS-1), RMGIC, RBC, and enamel surfaces displayed a complex multi-layered biofilm with a very high ratio of viable cells. HVGIC surfaces displayed a thinner biofilm with a higher ratio of dead cells, especially in close proximity to the surface. After 5 weeks of storage (group AS-5), no relevant differences in the biofilms were identified for RMGIC, RBC, and enamel specimens in comparison to group AS-1, while biofilms on the surface of HVGIC featured a lower ratio of dead cells.

Brushing with the fluoride-containing toothpaste (Group AS-5-brush) did not produce any changes in the biofilms growing on the RBC, while for RMGIC a reduction in the adherent biomass was identified; however, no effect on its viability was observed. For enamel, less dense biofilm structures with a higher ratio of dead cells were identified, and HVGIC displayed biofilms with the highest ratio of dead cells. Treatment with the highly concentrated fluoride solution (group AS-5-exp) had a similar effect on the biofilms developed on the HVGIC as in group AS-5-brush. Biofilms formed on RMGIC and enamel showed a higher ratio of dead cells in group AS-5-exp than in group AS-5-brush, while no relevant differences were identified between biofilms on RBC surfaces in all groups.

The results after simulation of biofilm formation in the multispecies model are displayed in Fig. 5c. Both material and treatment significantly influenced viable biomass ($p < 0.001$). No significant differences in viable biomass were identified between the treatment groups for the restorative materials HVGIC, RMGIC, and RBC, indicating that treatment with fluoride had no effect on viable biomass on the surface of these materials in the multispecies biofilm model. Viable biomass on enamel was significantly lower after treatment in accordance with group AS-5-brush and AS-5-exp protocols ($p < 0.005$).

3.3. *Release of fluoride*

The release of fluoride was significantly higher from HVGIC than from RMGIC; no release of fluoride was observed from the RBC as well as enamel (Fig. 7a). A relevant fluoride burst was identified for HVGIC and RMGIC; for RMGIC, the release of fluoride approached a plateau after a period of three weeks. Treatment with toothpaste in group AS-5-brush correlated with a significantly higher release of fluoride from HVGIC and RMGIC. Significant interaction effects were observed between the two factors, indicating that the release of fluoride depended on both material and treatment. Treatment with fluoride in groups AS-5-brush and AS-5-exp significantly reduced the decrease in the release of fluoride from the bioactive materials. For enamel, a significant and steadily increasing release of fluoride was observed following treatment with toothpaste in group AS-5-brush. Exposition to a solution with high a high concentration of fluoride in group AS-5-exp resulted in a high intake of fluoride by HVGIC and enamel (Fig. 7b).

For groups AS-1, AS-5, and AS-5-brush, high fluoride surface content correlated with high release of fluoride. The

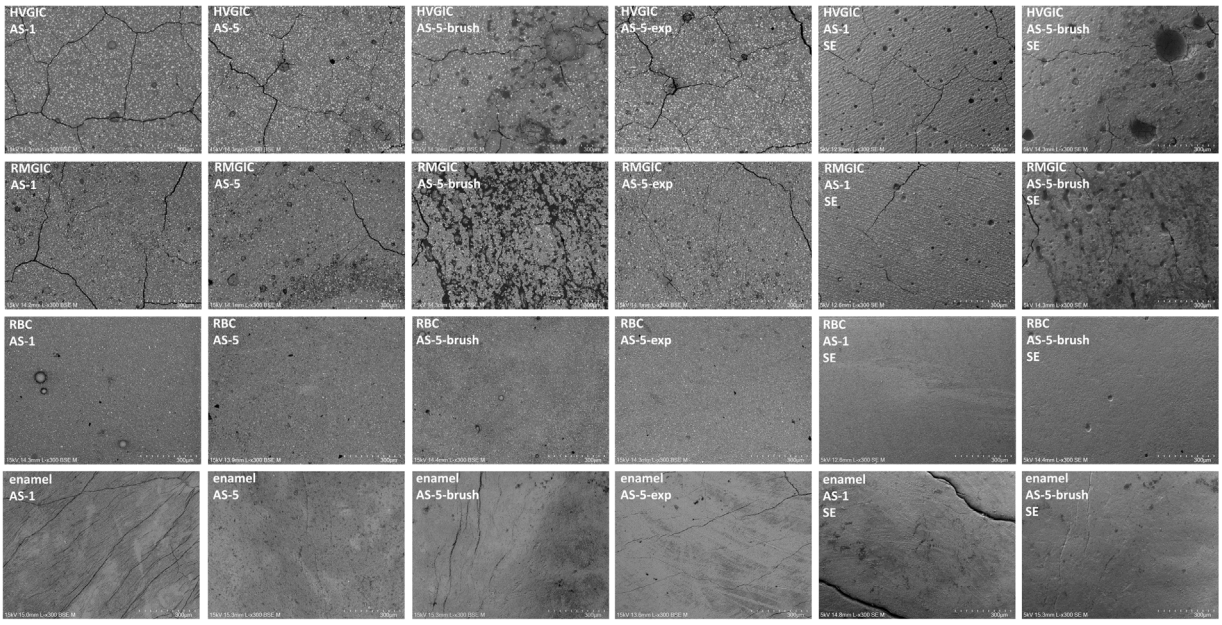

Fig. 3 – Scanning electron microscopic (SEM) analysis of the surface of the various materials. A representative microscopic field acquired in backscattered electron (BE) mode with an acceleration voltage of 15 kV and a magnification of 300× is displayed for each material and for each treatment group. RMGIC showed intermediate surface features between HVGIC and RBC materials. For both HVGIC and RMGIC surface cracks and bubbles incorporated during the mixing procedure can be identified. Due to its resin matrix, RMGIC showed less cracks and bubbles than HVGIC. To better display surface changes resulting from the brushing procedure, an additional set of images was acquired in secondary electron (SE) mode with an acceleration voltage of 5 kV and a magnification of 300 × . As in groups AS-1, AS-5, and AS-5-exp only little differences in surface morphology were identified for all materials, representative images of each material from treatment group AS-1 were compared to AS-5-brush. Brushing relevantly impacted the surface of RMGIC and, to a lesser extent, HVGIC. Brushing caused an abrasion of filler particles and, particularly for RMGIC, produced a surface mainly consisting of matrix. RBC and enamel materials showed very homogeneous surfaces that were not altered by the different treatments.

correlation is given by the equation Log(Fluoride release (ppb/mm^2)) = −0.505 + 1.048*Fluoride content(%), p = 0.744.

4. Discussion

The currents study hypothesized that (1) recharging restorative materials with fluoride decreases biofilm formation on their surface, and (2) the effect is dependent on time, biofilm, and material. The results suggest acceptance of the first research hypothesis as for some restorative materials a significant impact of treatment with fluoride on biofilm formation was identified. The second research hypothesis can also be accepted, as the effect of treatment with fluoride showed a relevant dependency on time, the material, and the microbiological model employed for simulation of biofilm formation.

Although a lot of effort is being put into novel developments, no direct restorative materials are currently available that guarantee successful replacement of natural tooth tissues for the whole life of the patient. While nanohybride RBCs feature several favorable properties such as easy handling as well as advantageous mechanics and esthetics, these materials also have some weaknesses, including the degradation of the adhesive interface by endogenous and exogenous factors. Moreover, RBCs do not feature a buffering capacity as natural tooth tissues do [19], which promotes the formation of cariogenic biofilms on their surface. In contrast, GICs are bioactive materials as they release biologically active ions such as fluoride, sodium, phosphate, and silicate into the surrounding tissues and may also absorb ions from saliva. The release of ions from GICs produces an ion-rich layer in the adjacent tooth tissues which is very resistant to acidic attack [4]. Moreover, it has been shown that the release of ions from GICs is relevantly increased in acidic environments [20], and a buffering effect of GICs has been proven [21]. As a result, it has been shown that these materials may prevent demineralization of adjacent natural tooth tissues [22,23] and cariogenic biofilm formation [24]. However, the release of fluoride follows a particular kinetic pattern, including an initial phase with a very high release (i.e. burst effect) which is followed by lower and steadily decreasing release of fluoride with time. It has been reported that the release of fluoride from restorative materials is a complex process, including the diffusion of water into the material, the dissolution or exchange of fluoride in the solid as well as the diffusion of fluoride out of the material [25]. In general, in the present study, a logarithmic correlation was identified between fluoride surface content and release. For GICs, the initial fluoride burst has been explained by the release of loosely bound fluoride in the matrix of the cement, while the following phase is caused by the continuous release of fluoride from the glass particles of the cement as a result of ion exchange [5]. Regarding the rate of fluoride released from

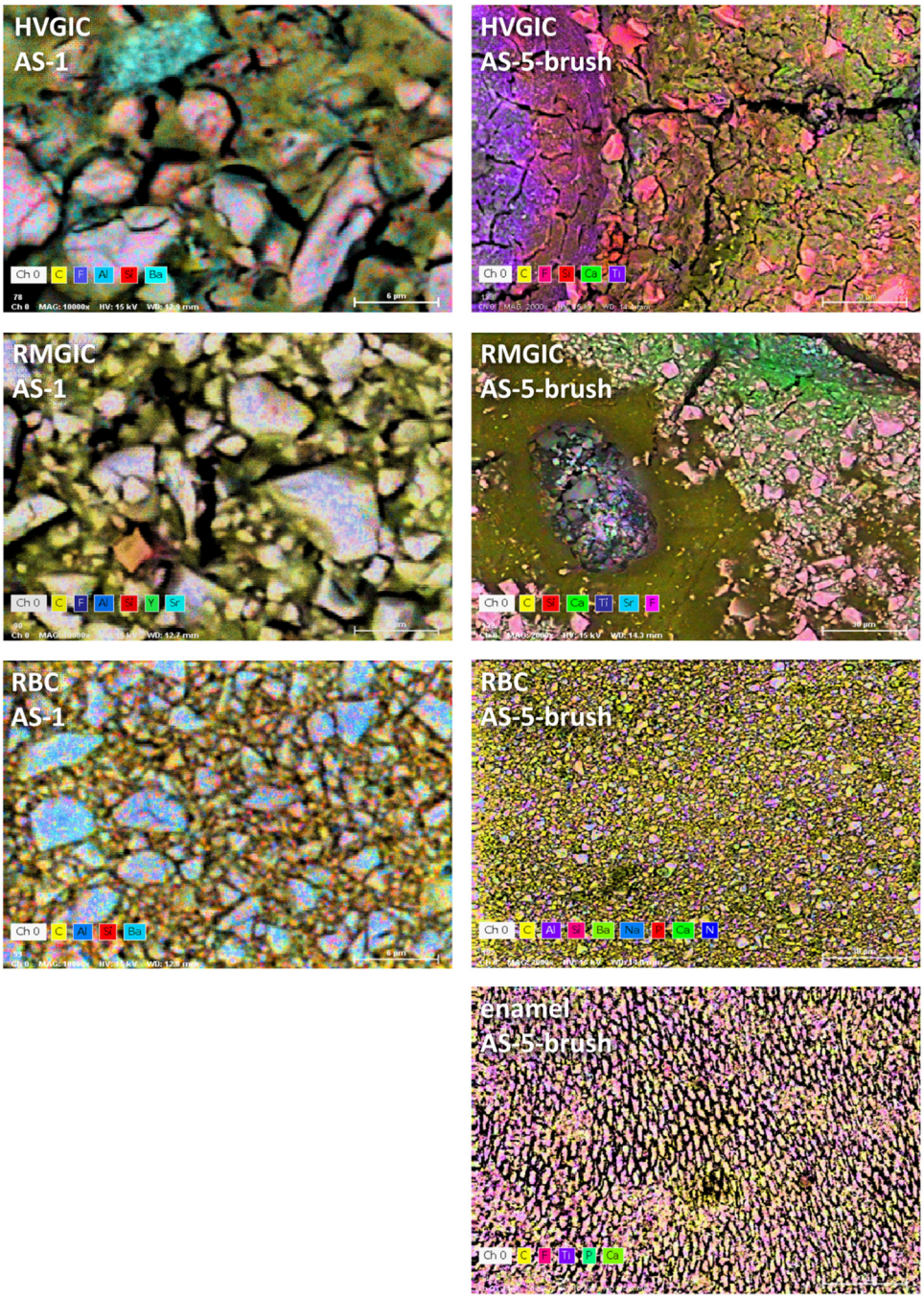

Fig. 4 – Energy-dispersive X-ray spectroscopy (EDS) maps displaying the distribution of elements on the surface of the various materials in group AS-1 (magnification 10,000×). A set of maps was acquired for all materials in group AS-5-brush at a magnification of 2000×, showing the deposition of foreign elements on the surface of the materials. In particular, Ti was identified on the bottom of bubbles and cracks in HVGIC and RMGIC as well as enamel, which resulted from the titanium containing toothpaste. For the RBC, the presence of other elements such as Ca, P, Na, and N was observed, which indicates that brushing can relevantly modify the elemental surface composition of a dental material in a very complex way.

resin-modified in comparison to conventional glass ionomer cements, controversial results have been published, which have been attributed to the materials selected, the experimental design as well as the storage medium [5,26,27]. The higher release of fluoride from HVGIC in comparison to RMGIC observed in the current study might be explained by the curing reaction of the RMGIC, which reduces the sensitivity against moisture [28]. Moreover, it might be possible that the diffusion of water into the cement is inhibited by the polymeric network of the RMGIC, which consequently impairs the elution of fluoride [29]. The results of the current study corroborate data from previous studies, indicating that HVGICs and RMG-

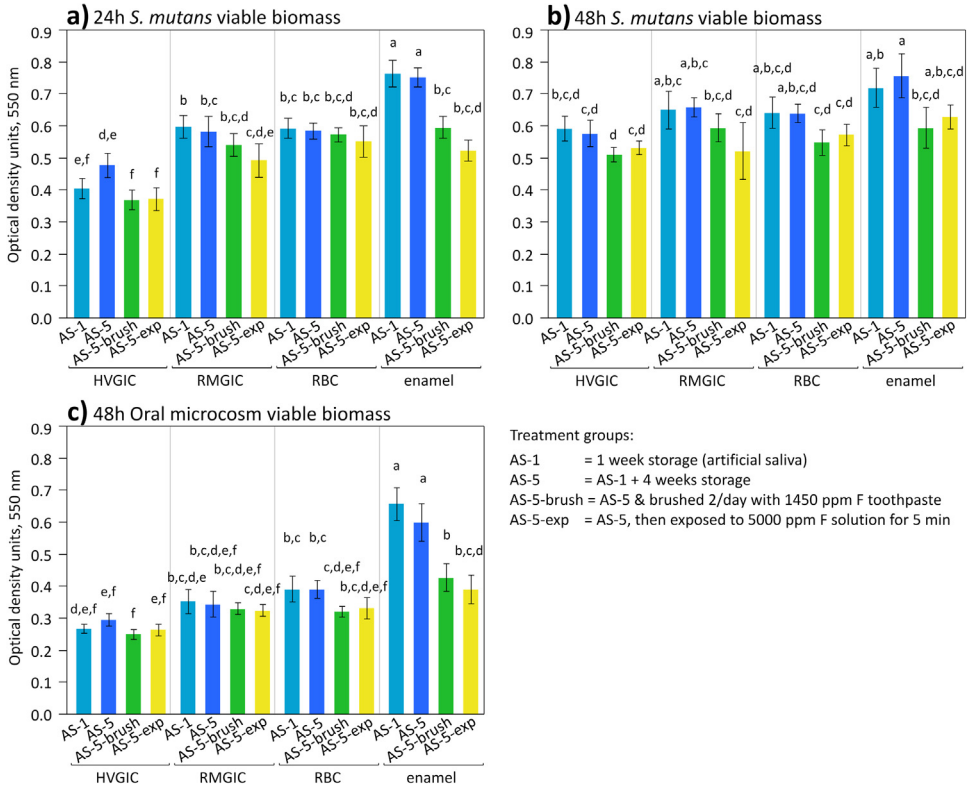

Fig. 5 – Biofilm formation (optical density units) on the various materials: (a) *S. mutans* biofilm formation after 24 h. (b) *S. mutans* biofilm formation after 48 h (c) Biofilm formation in the multispecies biofilm model after 48 h. Different superscript letters indicate statistically significant differences between groups (Tukey's test, $p < 0.05$).

ICs can be effectively recharged with fluoride by brushing with a fluoride-containing toothpaste or exposition to solutions with a high concentration of fluoride, although the levels of released fluoride did not approximate baseline values. Correlations between EDS data and the release of fluoride indicated that exposition to a solution with a high concentration of fluoride had a more distinct effect on the uptake of fluoride by the surface while brushing had a more pronounced effect in increasing the release of fluoride from HVGIC and RMGIC over time. Not surprisingly, no relevant levels of fluoride were released from the RBC, and treatments with fluoride did not produce any effect on the release of fluoride for this material. These observations corroborate previous data suggesting that only fluoride-containing RBCs can be recharged with fluoride [14]. Regardless of the microbiological model employed there was a tendency towards lower biofilm formation on HVGIC in comparison to RMGIC and RBC, while highest values were identified for enamel. However, in enamel specimens, treatments with fluoride produced a significant reduction in biofilm formation regardless of the microbiological model applied. While a similar tendency was identified for HVGIC and RMGIC, the effect of fluoride recharge on biofilm formation was less pronounced than for enamel and most prominent in the 24 h *S. mutans* microbiological model. Although the amount of biomass increased significantly with prolonged incubation times, CLSM analyses conducted for *S. mutans* biofilms after 48 h indicated the presence of a layer of predominantly dead bacterial cells adjacent to the surface of restorative materials that featured an initially relevant release of fluoride, while in the external layers of the biofilms a majority of viable microorganisms was identified. With regard to this aspect, previous studies from our groups indicated that the presence of biofilms on the surface of restorative materials significantly impacts the release of fluoride from the surface [12]. Moreover, it has recently been reported that repeated treatment of *S. mutans* biofilms with fluoride relevantly affected their composition and virulence, while overall biovolume was not affected. These observations were attributed to an inhibition of the production of extracellular polysaccharides [30]. A recent study highlighted that, for some *S. mutans* strains, fluoride may inhibit biofilm formation at concentrations of 100 ppm [31]. Although the levels of fluoride released from HVGIC and RMGIC were much lower than this threshold, recharging HVGIC and RMGIC with fluoride led to a significant decrease in biofilm formation in the *S. mutans* microbiological model after 24 h. In both microbiological models, differences were less pronounced after 48 h and did not meet statistical significance. These findings indicate that a release of fluoride is particularly relevant for the earlier phases of biofilm formation, which corroborates previously published results from our groups [12].

The data of the current study suggest that enamel can be charged with fluoride and produces a relevant release of fluoride; brushing was more effective in charging enamel surface with fluoride than exposition to a solution with a high concentration of fluoride. It has been reported that the

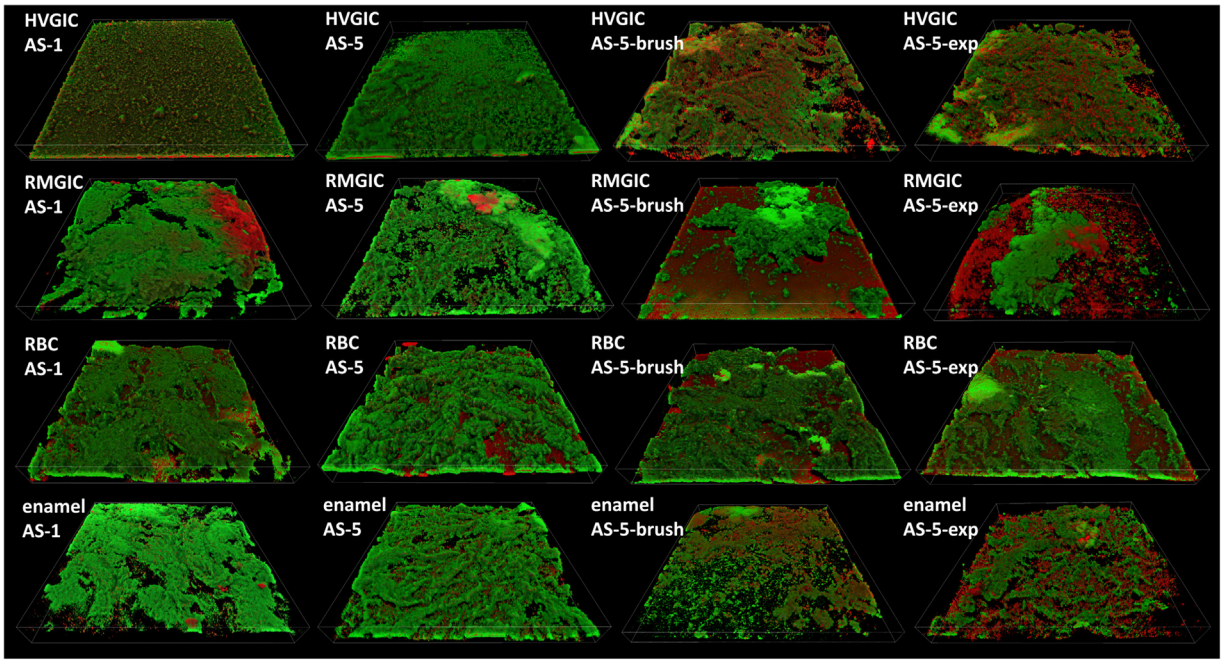

Fig. 6 – 3D confocal laser scanning microscopic (CLSM) reconstructions (750 μm × 750 μm fields) of *S. mutans* biofilms (48 h) on the surface of the various materials after the different treatments. Viable bacterial cells are displayed as green and dead bacterial cells as red. Autofluorescence from the surface can be identified in several fields, especially for RBC and RMGIC which is caused by the resin matrix. No relevant differences were identified between biofilms on RBC surfaces in all groups. In group AS-1, RMGIC, RBC, and enamel displayed a complex multi-layered biofilm with a very high ratio of viable cells. HVGIC surfaces showed a thinner biofilm with a higher ratio of dead cells, especially in close proximity to the surface. In group AS-5, biofilms on the surface of HVGIC featured a lower ratio of dead cells in comparison to group AS-1. In group AS-5-brush, HVGIC showed biofilms with the highest ratio of dead cells, while RMGIC showed a reduction in the adherent biomass but no reduction in viability. Less dense biofilm structures with a higher ratio of dead cells were identified on enamel. Treatment in group AS-5-exp had a similar effect on the biofilms on HVGIC as treatment in group AS-5-brush. Biofilms formed on RMGIC and enamel showed a higher ratio of dead cells in group AS-5-exp than in group AS-5-brush (For interpretation of the references to colour in this figure legend, the reader is referred to the web version of this article).

application of fluoride-containing dentifrices causes the precipitation of calcium fluoride-like material on the surface of enamel, which serves as a pH-driven fluoride reservoir [32]. Titty et al. analyzed mineral content of demineralized enamel that had been brushed with different toothpastes and subjected to pH-cycling for 4 weeks. The authors identified that fluoride-containing toothpastes significantly increased the fluoride content of enamel; however, measurements were performed only once at the end of the treatment period [33]. Interestingly, in the current study, the release of fluoride from enamel increased almost linearly over the whole treatment period in specimens that had been brushed with toothpaste. Thus, future and extended studies might further address this observation that may have translational importance on the advice for the usage of fluoride-containing toothpastes. However, the effect of both treatments on biofilm formation was equally significant after 24 h on *S. mutans* biofilm and after 48 h on mixed plaque. A reason for this behavior might be that biofilms are sensitive to the amount of fluoride released, and it could be speculated that the release might depend on the surface and the material. These observations indicate that enamel might serve as a fluoride reservoir that – if regularly recharged – relevantly impacts biofilm formation. Levels of fluoride released from enamel, were, however, markedly lower than for HVGIC and RMGIC, which indicates that not all factors influencing biofilm formation on enamel and dental restorative materials have yet been identified. Fernández et al. investigated the impact of SnF_2 and NaF toothpaste on *S. mutans* biofilms on enamel and showed that only treatment of biofilms with SnF_2 toothpaste significantly reduced biofilm mass and thickness [34]. This phenomenon has been attributed to an antimicrobial effect of stannous ions. However, the results of the current trial indicate that application of NaF-containing toothpastes may significantly impact biofilm formation on enamel.

EDS maps indicated that titanium particles from the toothpaste are transferred onto the surface of the various materials. While titanium dioxide has no antimicrobial effect in the absence of ultraviolet light, the data suggest that the surface composition is relevantly modified by tooth brushing procedures.

Surface roughness has been identified as the most important surface parameter that affects biofilm formation on dental restorative materials, and the conventional wisdom is that biofilm formation is increased on surfaces with high surface roughness [35]. With regard to this aspect, a thresh-

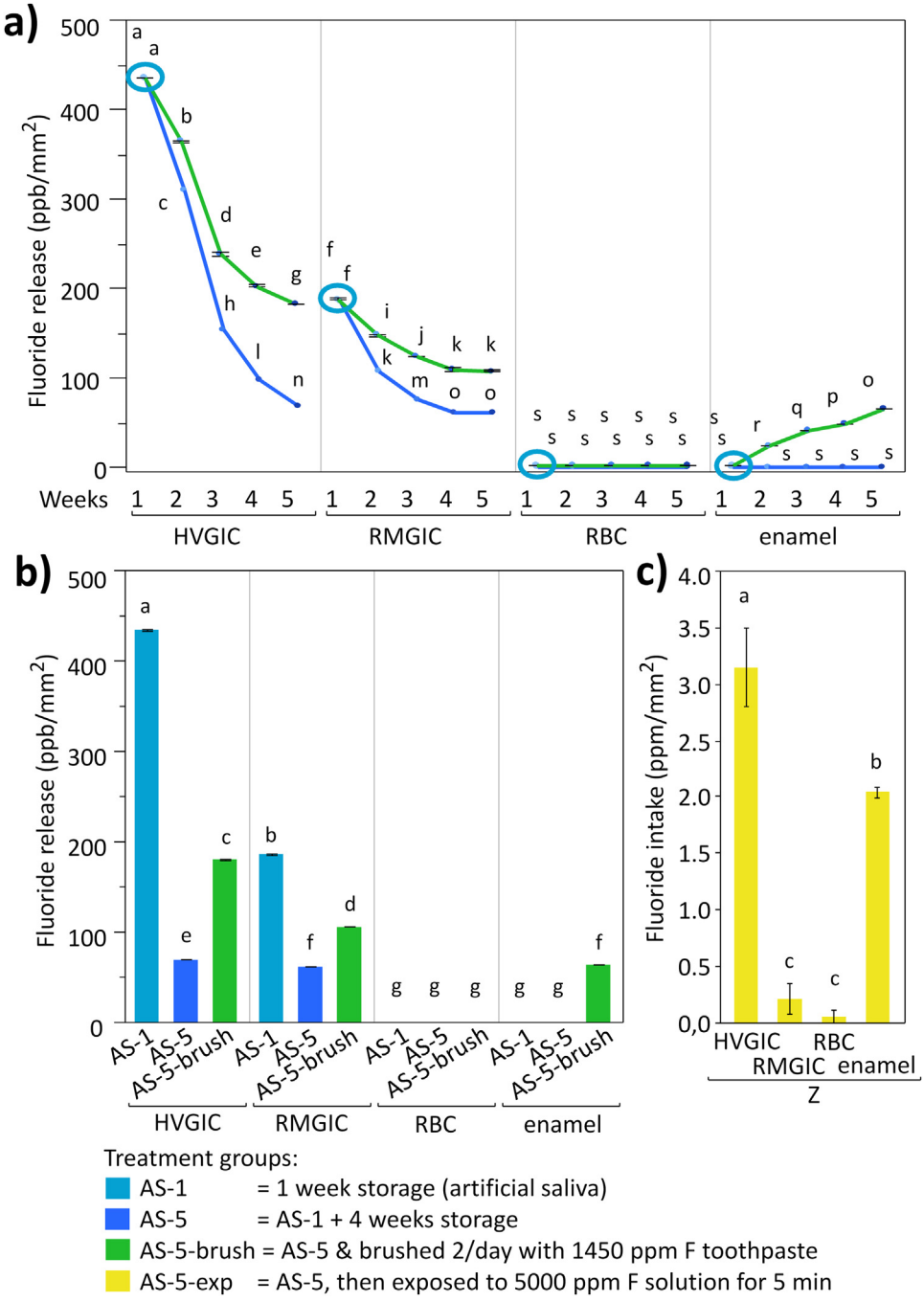

Fig. 7 – (a) Release of fluoride (ppb/mm²) identified for the treatment groups AS-5 and AS-5-brush after each week. The first time point refers to specimens measured after the first week of storage (AS-1), which was identical for all specimens and treatment groups. (b) Release of fluoride (ppb) at the last measurement point before submitting specimens to microbiological procedures. (c) Intake of fluoride in group AS-5-exp after treatment with the fluoride solution. The amount of intake (ppm/mm²) was calculated measuring the difference in fluoride content of the 50 mL solution containing 5000 ppm fluoride in which specimens were immersed for 5 min under constant stirring prior and after treatment of the specimens. In all graphs, different superscript letters indicate statistically significant differences between groups (Tukey's test, $p < 0.05$).

old value at 0.2 μm had been introduced in the past, implying that lower values for surface roughness do not further impact biofilm formation [36]. In the current trial, significantly higher surface roughness – which was markedly higher than the 0.2 μm threshold– was identified for HVGIC than for RBC, yet viable biomass was significantly lower on the glass ionomer material. This observation underlines that surface roughness is not the only parameter affecting biofilm formation on the surface of restorative materials and emphasizes the effect of fluoride released from the materials on biofilm formation.

Regarding the SEM technique employed for analysis of the surface of the materials, elements with high atomic number tend to yield a higher amount of backscattering, which is displayed as white spot in an image gathered by BE mode. Resin-based composites are regularly fabricated from fillers high atomic number (Si, Al, Ba, Sr) which are embedded in a matrix with low atomic number (C, O). Thus, it is particularly interesting to analyze these materials with the BE mode. Due to the type of electron interactions, the SE signal comes from a more superficial layer than BE electrons. Low acceleration voltages (5 kV) provide information from a superficial layer (500 nm or less), while higher voltages (15 kV) provide information deeper layers (1–1.5 μm). By selecting a low acceleration voltage in SE mode and correlating the image with sub-surface information gather by higher acceleration voltages in BE mode, it is possible to identify little surface modifications such as those resulting from brushing in the current study. Analysis of RMGIC after brushing (group AS-5-brush) with BE mode showed the presence of high amounts of elements with low atomic number, which were likely from organic origin. However, 5 kV images gathered in BE mode indicated that brushing caused an abrasion of filler particles from the material, producing a surface mainly consisting of resin matrix. While no relevant differences in surface roughness were identified, this observation might serve as an explanation why one-time recharge with a solution with high fluoride content reduced biofilm formation more efficiently than constant brushing that abraded the filler particles that could be recharged with fluoride.

The authors are aware that the data of the current trial have to be interpreted within the limitations of a laboratory study. Although natural biofilms on the surface of teeth and dental materials feature a complex variety of microorganisms, monospecies microbiological models feature the advantages of standardized and reproducible experimental conditions. *S. mutans* has been identified as one of the major causative agents of dental caries [37,38], which justifies its selection for application in the monospecies biofilm model. A recent study highlighted that the effect of fluoride on *S. mutans* biofilm formation is dependent on the bacterial strain employed [31], which indicates that a monospecies microbiological model with a single *S. mutans* strain cannot adequately address all aspects of interaction with fluoride released from dental materials. Thus, a multispecies microbiological model using pooled whole saliva from different volunteer donors was additionally employed which responds to the complex interactions between multiple microorganisms in the oral cavity and contributes to the significance and validity of the data gathered from this trial. Nevertheless, the data of the current trial should be corroborated by clinical studies as not all microorganisms can be adequately cultured in laboratory models.

5. Conclusion

The results of the current study highlight that treatment with fluoride-containing agents may relevantly affect biofilm formation on the surface of high-viscosity glass ionomer cements and enamel and – to a lesser extent – resin-modified glass ionomer cements, while no effect on biofilm formation on resin-based composites was identified. As the results showed a dependency on the experimental conditions and models applied clinical studies should be performed to corroborate these results.

Funding

The authors confirm that parts of this work were supported by VOCO GmbH, Cuxhaven, Germany.

Acknowledgements

The authors are grateful to Massimo Tagliaferro for providing access to the EDS analyses.

REFERENCES

[1] Rasines Alcaraz MG, Veitz-Keenan A, Sahrmann P, Schmidlin PR, Davis D, Iheozor-Ejiofor Z. Direct composite resin fillings versus amalgam fillings for permanent or adult posterior teeth. Cochrane Database Syst Rev 2014:CD005620.
[2] Skartveit L, Tveit B, Total B, Øvrebø R, Raadal M. In vivo fluoride uptake in enamel and dentin fluoride from containig materials. J Dent Child 1990;57:97–100.
[3] Mukai M, Ikeda M, Yanagihara T, Hara G, Kato K, Nagagaki M, et al. Fluoride uptake in human dentine from glass-ionomer cement in vivo. Arch Oral Biol 1993;38:1093–8.
[4] Sidhu SK, Nicholson JW. A review of glass-ionomer cements for clinical dentistry. J Funct Biomater 2016;7:16.
[5] Burke FM, Ray NJ, McConnell RJ. Fluoride-containing restorative materials. Int Dent J 2006;56:33–43.
[6] Wiegand A, Buchalla W, Attin T. Review on fluoride-releasing restorative materials—fluoride release and uptake characteristics, antibacterial activity and influence on caries formation. Dent Mater 2007;23:343–62.
[7] Busscher HJ, Rinastati M, Siswomihardjo W, van der Mei HC. Biofilm formation on dental restorative and implant materials. J Dent Res 2010;89:657–65.
[8] Brambilla E, Cagetti MG, Gagliani M, Fadini L, García-Godoy F, Strohmenger L. Influence of different adhesive restorative materials on mutans Streptococci colonization. Am J Dent 2005;18:173–6.
[9] Andrucioli MCD, Faria G, Nelson-Filho P, Romano FL, Matsumoto MAN. Influence of resin-modified glass ionomer and topical fluoride on levels of *Streptococcus mutans* in saliva and biofilm adjacent to metallic brackets. J Appl Oral Sci 2017;25:196–202.
[10] Chau NPT, Pandit S, Cai JN, Lee MH, Jeon JG. Relationship between fluoride release rate and anti-cariogenic biofilm activity of glass ionomer cements. Dent Mater 2015;31:e100–8.
[11] Hahnel S, Wastl DS, Schneider-Feyrer S, Giessibl FJ, Brambilla E, Cazzaniga G, et al. *Streptococcus mutans* biofilm formation and release of fluoride from experimental resin-based composites depending on surface treatment and S-PRG filler particle fraction. J Adhes Dent 2014;16:313–21.
[12] Hahnel S, Ionescu AC, Cazzaniga G, Ottobelli M, Brambilla E. Biofilm formation and release of fluoride from dental restorative materials in relation to their surface properties. J Dent 2017;60:14–24.
[13] Gandolfi MG, Chersoni S, Acquaviva GL, Piana P, Prati C, Mongiorgi R. Fluoride release and absorption at different pH from glass-ionomer cements. Dent Mater 2006;22:441–9.

[14] Naoum S, Ellakwa A, Martin F, Swain M. Fluoride release, recharge and mechanical property stability of various fluoride-containing resin composites. Oper Dent 2011;36–4:422–32.
[15] Arvidsson K, Johansson EG. Galvanic currents between dental alloys in vitro. Scand J Dent Res 1995;93:467–73.
[16] Guggenheim B, Giertsen E, Schupbach P, Shapiro S. Validation of an in vitro biofilm model of supragingival plaque. J Dent Res 2001;80:363–70.
[17] Ionescu AC, Brambilla E, Travan A, Marsich E, Donati I, Gobbi P, et al. Silver-polysaccharide antimicrobial nanocomposite coating for methacrylic surfaces reduces *Streptococcus mutans* biofilm formation in vitro. J Dent 2015;43:1483–90.
[18] Ionescu A, Wutscher E, Brambilla E, Schneider-Feyrer S, Giessibl FJ, Hahnel S. Influence of surface properties of resin-based composites on in vitro *Streptococcus mutans* biofilm development. Eur J Oral Sci 2012;120:458–65.
[19] Nedeljkovic I, De Munck J, Slomka V, Van Meerbeek B, Teughels W, Van Landuyt KL. Lack of buffering by composites promotes shift to more cariogenic bacteria. J Dent Res 2016;95:875–81.
[20] Nicholson JW, Czarnecka B. Role of aluminum in glass-ionomer dental cements and its biological effects. J Biomater Appl 2009;24:293–308.
[21] Nicholson JW, Czarnecka B, Limanowska-Shaw H. The long-term interaction of dental cements with lactic acid solutions. J Mater Sci Mater Med 1999;10:449–52.
[22] Cury JA, De Oliveira BH, Dos Santos APP, Tenuta LMA. Are fluoride releasing dental materials clinically effective on caries control? Dent Mater 2016;32:323–33.
[23] Tedesco TK, Bonifácio CC, Calvo AFB, Gimenez T, Braga MM, Raggio DP. Caries lesion prevention and arrestment in approximal surfaces in contact with glass ionomer cement restorations—a systematic review and meta-analysis. Int J Paediatr Dent 2016;26:161–72.
[24] Chau NPT, Pandit S, Jung J-E, Cai J-N, Yi H-K, Jeon J-G. Long-term anti-cariogenic biofilm activity of glass ionomers related to fluoride release. J Dent 2016;47:34–40.
[25] Yap AUJ, Khor E, Foo S. Fluoride release and antibacterial properties of new-generation tooth-colored restoratives. Oper Dent 1999;24:297–305.
[26] Kan KC, Messer LB, Messer HH. Variability in cytotoxicity and fluoride release of resin-modified glass-ionomer cements. J Dent Res 1997;76:1502–7.
[27] Al-Naimi OT, Itota T, Hobson RS, McCabe JF. Fluoride release for restorative materials and its effect on biofilm formation in natural saliva. J Mater Sci Mater Med 2008;19:1243–8.
[28] Wilson AD. Resin-modified glass-ionomer cements. Int J Prosthodont 1990;3:425–9.
[29] Mathis RS, Ferracane JL. Properties of a glass-ionomer/resin-composite hybrid material. Dent Mater 1989;5:355–8.
[30] Pandit S, Jung JE, Choi HM, Jeon JG. Effect of brief periodic fluoride treatments on the virulence and composition of a cariogenic biofilm. Biofouling 2017;34:53–61.
[31] Nassar HM, Gregory RL. Biofilm sensitivity of seven *Streptococcus mutans* strains to different fluoride levels. J Oral Microbiol 2017;9:1328265.
[32] Lussi A, Carvalho TS. The future of fluorides and other protective agents in erosion and prevention. Caries Res 2015;49(Suppl. 1):18–29.
[33] Titty TM, Shrikrishna SB, Rao A, Shenoy R, Natarajan S. Remineralizing effectiveness of calcium sucrose phosphate and fluoride dentifrices: an in vitro study. Contemp Clin Dent 2018;9:276–82.
[34] Fernández CE, Fontana M, Smaraian D, Cury JA, Rickard AH, González-Cabezas C. Effect of fluoride-containing toothpastes on enamel demineralization and *Streptococcus mutans* biofilm architecture. Caries Res 2016;50:151–8.
[35] Teughels W, van Assche N, Sliepen I, Quirynen M. Effect of material characteristics and/or surface topography on biofilm development. Clin Oral Impl Res 2006;17(Suppl. 2):68–81.
[36] Bollen CM, Lambrechts P, Quirynen M. Comparison of surface roughness of oral hard materials to the threshold surface roughness for bacterial plaque retention: a review of the literature. Dent Mater 1997;13:258–69.
[37] De Stoppelaar JD, van Houte J, Backer Dirks O. The relationship between extracellular polysaccharide-producing streptococci and smooth surface caries in 13-year-old children. Caries Res 1990;3:190–9.
[38] Forssten SD, Bjorklund M, Ouwehand AC. *Streptococcus mutans*, caries and simulation models. Nutrients 2010;2:290–8.